arXiv:0906.5600v1 [cond-mat.mes-hall] 30 Jun 2009

Interface States in Carbon Nanotube Junctions: Rolling up graphene

H. Santos[1], A. Ayuela[2], W. Jaskólski[3], M. Pelc[3], and L. Chico[1]
[1] *Instituto de Ciencia de Materiales de Madrid, CSIC, Cantoblanco, 28049 Madrid, Spain*
[2] *Centro de Física de Materiales CSIC-UPV/EHU, Departamento de Física de Materiales (Facultad de Químicas), and Donostia International Physics Center (DIPC), 20080 Donostia, Spain and*
[3] *Instytut Fizyki UMK, Grudziadzka 5, 87-100 Toruń, Poland*
(Dated: June 30, 2009)

We study the origin of interface states in carbon nanotube intramolecular junctions between achiral tubes. By applying the Born-von Karman boundary condition to an interface between armchair- and zigzag-terminated graphene layers, we are able to explain their number and energies. We show that these interface states, costumarily attributed to the presence of topological defects, are actually related to zigzag edge states, as those of graphene zigzag nanoribbons. Spatial localization of interface states is seen to vary greatly, and may extend appreciably into either side of the junction. Our results give an alternative explanation to the unusual decay length measured for interface states of semiconductor nanotube junctions, and could be further tested by local probe spectroscopies.

PACS numbers:

Carbon nanotubes are currently regarded as one of the most promising materials to develop future nanoelectronics, with an impressive combination of robustness and ideal electronic properties. At present, it is well established that further progress towards real applications depends on the ability to form junctions between different nanotubes [1]. Recently, the controlled synthesis of several carbon nanotube intramolecular junctions has been reported, either by current injection between nanotubes [2] or by temperature changes during growth [3]. These intramolecular junctions, which often present interface states, are typically made of topological defects arising from the connection between tubes of different chirality. In fact, the interplay between defects and charge transport is a central theme of carbon nanotubes (CNT) research in the fabrication of electronic devices, such as diodes [4] or transistors [5].

Although interface states are commonly regarded as a drawback in device performance, they may actually provide a means of achieving diode behavior at the nanoscale, as proposed in Ref. [6]. In any case, transport spectroscopy experiments have shown that interface states play an important role in the behavior of CNT junctions [7, 8, 9]. On the one hand, Ishigami *et al.* studied interface states in metal/metal CNT junctions with scanning tunneling microscopy, showing that interface states extended approximately 2 nm from the junction [8]. On the other hand, Kim *et al.* found longer decay lengths for semiconductor nanotube junctions, with different values at each side of the interface [9]. Therefore, understanding the physics of CNT intramolecular junctions, for which interface states may dominate transport properties, has been a subject of growing activity in the last few years [10, 11, 12, 13, 14].

The main purpose of this letter is to describe interface states and elucidate their origin by studying junctions of varying diameter. Specifically, we address the energy spectra of achiral nanotube intramolecular junctions. Zigzag/armchair junctions are made by joining a $(2n, 0)$ and an (n, n) tube; this is achieved with a ring of n pentagon-heptagon defect pairs. In Fig. 1 we show a particular example of this kind of junctions, namely the (10,0)/(5,5) case, with a ring of 5 pentagon-heptagon (5/7) defects forming the union between the tubes. All calculations have been performed within the π-electron tight-binding approximation [15] and a Green function matching technique [12]. We have recently shown that for multiple junctions, like $N(12, 0)/M(6, 6)$ superlattices, this approximation yields the electronic structure around the Fermi energy (E_F) in good agreement with the results from first-principles calculations [16].

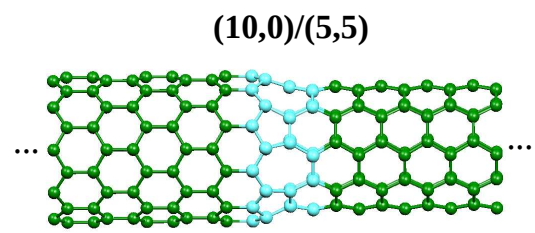

FIG. 1: (Color online) Geometry of a $(10, 0)/(5, 5)$ junction, with the atoms comprising the ring of pentagon-heptagon defects in a different color.

In Figure 2 we show the local density of states (LDOS) around E_F evaluated at the junction, for all $(2n, 0)/(n, n)$ systems from $n = 4$ to $n = 15$. The first interface state appears for $n = 4$; smaller junctions, such as the $(6, 0)/(3, 3)$ case (not shown), have no localized states even though they have a full ring of 5/7 topological defects. Clearly, interface states (IS) obey a multiple-of-three rule: when $n = 3q + 1$, with $q = 1, 2, ...$ a new interface state appears, q being the number of such states. Each interface state can be labeled by an integer number m, characterizing the behavior of the wavefunction Ψ_{IS} under rotations C_n of an angle $\phi = 2\pi/n$. As the junction

is invariant under C_n, it follows that $C_n\Psi_{IS} = e^{im\phi}\Psi_{IS}$. In Fig. 2 interface states of equal m are joined with a dashed line. The label m can be viewed as a "discrete angular momentum" quantum number [12]. The behavior of interface states is reminiscent of localized states in a quantum well system with increasing number of layers [17]. However, in contradistinction to quantum well states, these interface peaks cross with increasing system size. Another key feature is that their energies are limited to a narrow interval below E_F, specifically, between -0.3 and 0 eV, as can be seen in the Figure.

Additionally, notice that some interface states at junctions with different n have exactly the same energies. Such are, for example, the $(8,0)/(4,4)$, the $(16,0)/(8,8)$ and the $(24,0)/(12,12)$ junctions, which have one interface state at -0.172 eV, the $(12,0)/(6,6)$ and the $(24,0)/(12,12)$ junctions, with one IS at -0.285 eV. The coincidence in energies for some interface states and the regularity in their appearance point towards their folding origin. Thus, we have turned to a system closely related to this series of nanotube junctions: a semiinfinite zigzag graphene joined to an armchair-terminated one, yielding an infinite line of pentagon-heptagon topological defects as interface between the two graphene edges. The geometry of this graphene junction is shown in Fig. 3. In the same way that a perfect nanotube is made by rolling up a graphene sheet, a carbon nanotube junction like those described above can be obtained by rolling up a strip of these matched semiinfinite graphenes.

The bandstructure of the graphene armchair/zigzag interface is shown in the left panel of Fig. 4, along with the projected bulk bands at this interface; the right panel depicts the edge band of zigzag-terminated graphene with the corresponding projected graphene bulk bandstructure at this surface. The interface band shown in the left panel spans from Γ to 2/3 of the positive part of the Brillouin zone. Note that just at the edge points there are no interface states, because they belong to the bulk of the armchair- and the zigzag-terminated graphene respectively. The graphene interface band spans from -0.3 eV to 0 eV, comprising the energy range of all the nanotube interface states. Rolling up the graphene junction amounts to imposing Born-von Karman boundary condition to the graphene interface band. This determines the quantization rule

$$k = \frac{2\pi m}{nd}, \quad m = 0, ..., n-1, \tag{1}$$

where d is the length of the repeat unit along the interface and n is the number of repetitions to give a $(2n,0)/(n,n)$ junction. The index m is the same "discrete angular momentum" label formerly introduced. The allowed k values give the nanotube interface states shown in Fig. 2, as demonstrated graphically for two examples, namely $n = 5$ and $n = 9$, in the bottom panel of Fig. 4. The energies obtained by this rule exactly match those obtained in the nanotube junction calculations, collected in Fig. 2. The multiple-of-three periodicity is thus understood, due to the length of the BZ portion in which the

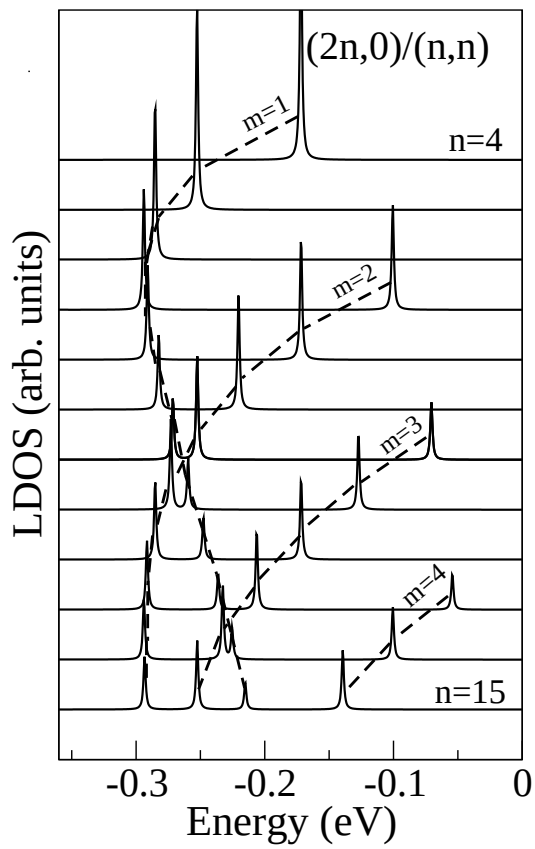

FIG. 2: Local density of states below the Fermi level vs n for a series of $(2n,0)/(n,n)$ junctions. Peaks correspond to interface states. The curves are arranged from top to bottom in order of increasing n, with the smallest and largest values indicated therein. Dashed lines are guides to the eye.

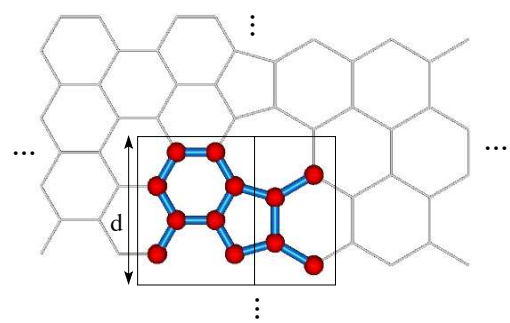

FIG. 3: (Color online) Geometry of the zigzag/armchair graphene junction. The two rectangles show the unit cells employed in the Green function matching calculation of interface bands.

interface graphene band exists, *i.e.*, 2/3 of its irreducible part. Furthermore, within the model employed, it is now clear why for $n < 4$ there are no interface states in the $(2n,0)/(n,n)$ junctions: in these cases, quantization lines touch the edges of the graphene interface band, and these end points do not actually belong to it because they are

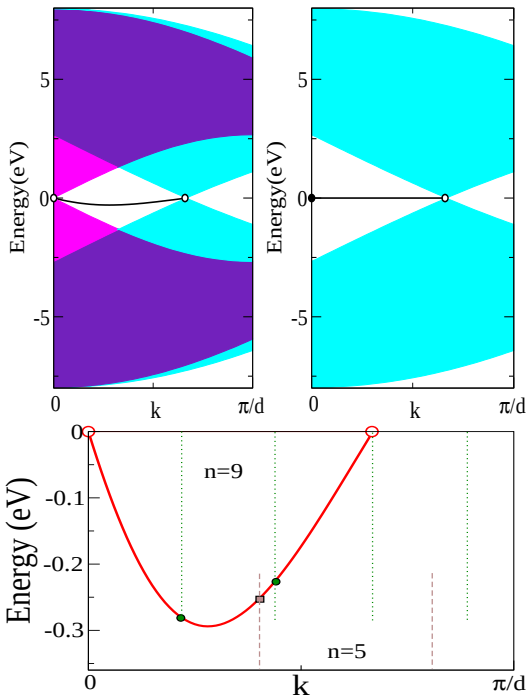

FIG. 4: Left panel: Interface band of the zigzag/armchair graphene junction, with the corresponding projected graphene bulk bands at this interface. Right panel: Edge band of the zigzag-terminated graphene with the graphene bandstructure projected at this surface. Bottom panel: Zoom of the interface band, with quantization lines showing the interface energies for the $n = 5$ (dashed) and the $n = 9$ junctions (dotted). Symbols mark the corresponding interface state energies. Open circles at the interface band ends stress that these energies do not belong to the band but, rather, to the bulk continua.

in the zigzag and armchair graphene bulk continua. Finally, the appearance of interface states with exactly the same energies is simply explained by the quantization rule given in Eq. (1).

To understand the origin of the interface band found for the zigzag/armchair graphene junction, we have analyzed the corresponding graphene free "surfaces", the armchair-terminated and the zigzag-terminated semiinfinite graphenes [18]. No surface bands appear in the gap of the armchair-terminated graphene, whereas for the zigzag-terminated one, shown in the right panel of Fig. 4, a flat band at 0 eV spans from Γ to 2/3 of the irreducible part of the BZ. For the purposes of direct comparison, we use the same unit cell as for the interface calculation, which is doubled with respect to the one usually employed for zigzag geometry. Note that the $k = 0$ state belongs to the surface band, given that it is in the bulk gap; this explains why all semiinfinite $(2n, 0)$ zigzag nanotubes have a "surface" edge state at 0 eV. Joining the zigzag edge graphene to the armchair one breaks the electron-hole symmetry due to the mixing of the two graphene sublattices, combing the surface band and moving it to negative energies, as depicted in the left panel of Fig. 4. Thus, the armchair-edge graphene acts as an external potential for the states of the zigzag-terminated graphene, bending down the interface band. The zigzag edge nature of the interface band shown in Fig. 4 is thus demonstrated, as well as that of interface states in zigzag/armchair junctions of tubes, which we have shown here to originate from edge states, as those found in graphene nanoribbons. This finding has implications for the analysis of other defects such as vacancies, and even substitutional atoms in nanotubes or graphene, which have been shown to yield an effective edge in the hexagonal carbon lattice [19].

In order to test the robustness of our tight-binding results, we have performed *ab initio* calculations of $4(2n, 0)/4(n, n)$ superlattices (SL) using the same method and parameters as in Ref. [16]. Introducing another junction and imposing periodic boundary conditions induces significant changes in the electronic structure, but by comparison to tight binding results and checking the wavefunction symmetry and spatial distribution, we have successfully identified interface states [20]. Specifically, we have checked that there are no interface states in the $(6, 0)/(3, 3)$ system, whereas one IS per junction appears in the $(8, 0)/(4, 4)$ and the $(12, 0)/(6, 6)$ cases, and two states per junction appear in the $(14, 0)/(7, 7)$ system. For the time being, further studies for lattices with a larger number of defects are beyond our computational capabilities. Hitherto, *ab initio* calculations and tight-binding results fully agree as to the number of interface states in these achiral junctions.

We have chosen a pair of interface states belonging to the largest system calculated by *ab initio* techniques, namely the $4(14, 0)/4(7, 7)$ SL, to show their spatial distribution. Their wavefunctions are shown in Fig. 5 (a). The lowest-lying interface state, labeled I1, is mainly localized at the interface, spreading towards the armchair side. This behavior was also observed in the interface states of $(12, 0)/(6, 6)$ SLs and $(10, 0)/(5, 5)$ junctions [6, 20]. But, surprisingly, the second interface state (labeled I2) spreads from the interface into the zigzag part. To understand these disparate behaviors, we turn back to the graphene junction. Fig. 5 (b) depicts the electron density of several graphene interface states with different k values; states are labeled with the corresponding k value in π/d units. When moving from Γ to the interface band edge at 2/3 of the BZ, the wavefunction localization changes from the armchair to the zigzag side; for k at the band minimum the wavefunction is mainly localized at the junction. This explains why the interface state of the $(12, 0)/(6, 6)$ junction, which stems from the graphene $k = 1/3$ state, is rather localized at the interface. Thus, the junctions with sufficiently large diameter will have different interface states spreading at opposite sides of the interface, but pinned at the carbon ring made of 5/7 topological defects.

Our results provide an alternative explanation to the unequal decay lengths found in semiconductor nanotube junctions, as well as to their large value compared to

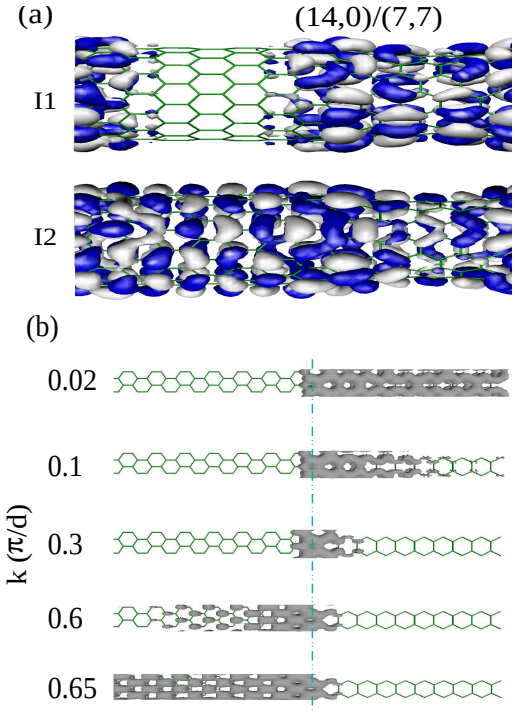

FIG. 5: (Color online) (a): Two examples of wavefunctions of interface states belonging to the $4(14,0)/4(7,7)$ superlattice calculated *ab initio*. (b): Electron density of several states belonging to the interface band of the graphene armchair/zigzag junction, calculated with a π-orbital tight-binding model.

metallic systems [8, 9]. The coexistence in the same nanotube of interface states with dissimilar spatial localization could be demonstrated by scanning tunneling microscopy and spectroscopy, as in Refs. [7, 8, 9]. The fact that CNT junctions may have several interface states with different spatial localizations opens a way for new device design based on their characteristics. Choosing a CNT of appropriate diameter, states with quite different spatial localization can be accessed by applying different voltages, allowing for switch operation. Furthermore, due to interface charge localization and redistribution CNT junctions can act as chemically active sites. Actually, doping the interfaces may induce a structural reconstruction and alter their symmetry, thus dramatically changing the electronic properties because of the Fermi level proximity to the IS.

Finally, although we have focused on junctions between achiral tubes and found that their interface states have zigzag edge origin, we would like to note that differences in chirality of joined tubes plays a role. For example, a zigzag (8,0)/(7,1) junction has no interface states, while the (8,0)/(5,3) junction has two [10]. We have chosen to study junctions between tubes with maximum difference in chiral angles. The non-trivial role of chirality deserves further exploration; but in any case, our present results suggest that IS in chiral systems will also have edge origin.

In summary, we have explored the nature of interface states in carbon nanotube junctions, focusing on achiral systems. We have shown that these states, usually attributed to the pentagon-heptagon topological defects, are actually due to the zigzag-edge-terminated nanotube. Topological defects break the electron symmetry and consequently make these states energy-dependent. Furthermore, we have related these interface states of nanotube junctions to the interface band appearing in a graphene zigzag/armchair junction. By applying the Born-von Karman boundary condition to the graphene interface band, we have derived the energies and number of the nanotube interface states, obtaining complete quantitative agreement with the CNT junction calculations. Our results give a new vision on the nature of CNT interface states and have implications in other systems, such as graphene vacancies or substitutional impurities.

L. C. acknowledges helpful discussions with J. I. Cerdá. This work has been partially supported by the Spanish DGES under grants MAT2006-06242 and FIS2007-66711-C02-C01 and Spanish CSIC under Grant PI 200860I048. W. J. and M. P. acknowledge financial support from Polish LFPPI.

[1] D. Wei, and Y. Liu, Adv. Mater. **20**, 2815 (2008).
[2] C. Jin, K. Suenaga, and S. Iijima, Nature Nanotech. **3**, 17 (2008).
[3] Y. Yao, Q. Li, J. Zhang, R. Liu, L. Jiao, Y. T. Zhu, and Z. Liu, Nature Mater. **6**, 283 (2007).
[4] P. G. Collins, A. Zettl, H. Bando, A. Thess, and R. E. Smalley, Science **278** 100 (1997); J. U. Lee, P.P. Gipp, and G.M. Heller, Appl. Phys. Lett. **85**, 145 (2004).
[5] S. J. Tans, A.R. M. Verschueren, and C. Dekker, Nature (London) **393**, 49 (1998); Z. Chen, J. Appenzeller, Y.-M- Lin, J. Sippel-Oakley, A. G. Rinzler, J. Tang, S. J. Wind, P. M. Solomon, and Ph. Avouris, Science **311**, 1735 (2006).
[6] A. Rochefort, and Ph. Avouris, Nano Lett. **2**, 253 (2002).
[7] H. Kim, J. Lee, S.-J. Kahng, Y.-W. Son, S. B. Lee, C.-K. Lee, J. Ihm, and Y. Kuk, Phys. Rev. Lett. **90**, 216107 (2003).
[8] M. Ishigami, H. J. Choi, S. Aloni, S. G. Louie, M. L. Cohen, and A. Zettl, Phys. Rev. Lett. **93**, 196803 (2004).
[9] H. Kim, J. Lee, S. Lee, Y. Kuk, J.-Y. Park, and S.-J. Kahng, Phys. Rev. B **71**, 235402 (2005).
[10] L. Chico, V. H. Crespi, L. X. Benedict, S. G. Louie, and M. L. Cohen, Phys. Rev. Lett. **76**, 971 (1996).
[11] R. Saito, G. Dresselhaus, and M. S. Dresselhaus, Phys. Rev. B **53**, 2044 (1996); J. C. Charlier, Ph. Lambin, and T. W. Ebbesen, Phys. Rev. B **53**, 11108 (1996).
[12] L. Chico, L. X. Benedict, S. G. Louie, and M. L. Cohen, Phys. Rev. B **54**, 2600 (1996).

[13] L. Chico, M. P. López Sancho, and M. C. Muñoz, Phys. Rev. Lett. **81**, 1278 (1998); C. G. Rocha, T. G. Dargam, and A. Latgé, Phys. Rev. B **65**, 165431 (2002); W. Zhang, W. Lu, and E. G. Wang, Phys. Rev. B **72**, 075438 (2005); F. Triozon, P. Lambin, and S. Roche, Nanotechnology **16** 230 (2005). E. Jódar, A. Pérez-Garrido, and A. Díaz-Sánchez, Phys. Rev. B **73**, 205403 (2006).

[14] L. Chico and W. Jaskólski, Phys. Rev. B **69**, 085406 (2004); W. Jaskólski, L. Chico, Phys. Rev. B **71**, 155305 (2005).

[15] With one π orbital per atom, the hopping parameter for nearest neighbors is fixed to $V_{pp\pi} = -2.66$ eV.

[16] A. Ayuela, L. Chico, and W. Jaskólski, Phys. Rev. B **77**, 085435 (2008).

[17] J. E. Ortega and F. J. Himpsel, Phys. Rev. Lett. **69**, 844 (1992); A. Ayuela, E. Ogando, and N. Zabala, Phys. Rev. B **75**, 153403 (2007).

[18] M. Fujita, K. Wakabayashi, K. Nakada, and K. Kusakabe, J. Phys. Soc. Jpn. **65**, 1920 (1996); K. Wakabayashi, M. Fujita, A. Ajiki, and M. Sigrist, Phys. Rev. B **59**, 8271 (1999).

[19] Y. Gan, L. Sun, and F. Banhart, Small **4**, 587 (2008).

[20] A. Ayuela, W. Jaskolski, M. Pelc, H. Santos, and L. Chico, Appl. Phys. Lett. **93**, 133106 (2008).